MOLECULAR AND CELLULAR BIOLOGY, July 2004, p. 5788–5796 Vol. 24, No. 13
0270-7306/04/$08.00+0 DOI: 10.1128/MCB.24.13.5788–5796.2004

Rhes Is Involved in Striatal Function

Daniela Spano,[1] Igor Branchi,[2] Annamaria Rosica,[1] Maria Teresa Pirro,[1] Antonio Riccio,[1] Pratibha Mithbaokar,[1] Andrea Affuso,[3] Claudio Arra,[3] Patrizia Campolongo,[2] Daniela Terracciano,[4] Vincenzo Macchia,[4] Juan Bernal,[5] Enrico Alleva,[2] and Roberto Di Lauro[1]*

Stazione Zoologica Anton Dohrn, Villa Comunale, 80121 Naples,[1] Section of Behavioural Neurosciences, Dipartimento di Biologia Cellulare e Neuroscienze, Istituto Superiore di Sanità, 00161 Rome,[2] Istituto Nazionale per lo Studio e la Cura dei Tumori Pascale, 80131 Naples,[3] and Dipartimento di Biologia e Patologia Cellulare e Molecolare L. Califano, Università degli Studi di Napoli Federico II, I-80131 Naples,[4] Italy, and Instituto de Investigaciones Biomédicas, 28029 Madrid, Spain[5]

Received 1 August 2003/Returned for modification 16 September 2003/Accepted 5 April 2004

The development and the function of central nervous system depend on thyroid hormones. In humans, the lack of thyroid hormones causes cretinism, a syndrome of severe mental deficiency. It is assumed that thyroid hormones affect the normal development and function of the brain by activating or suppressing target gene expression because several genes expressed in the brain have been shown to be under thyroid hormone control. Among these, the *Rhes* gene, encoding a small GTP-binding protein, is predominantly expressed in the striatal region of the brain. To clarify the role of *Rhes* in vivo, we disrupted the *Rhes* gene by homologous recombination in embryonic stem cells and generated mice homozygous for the *Rhes* null mutation (Rhes$^{-/-}$). *Rhes*$^{-/-}$ mice were viable but weighed less than wild-type mice. Furthermore, they showed behavioral abnormalities, displaying a gender-dependent increase in anxiety levels and a clear motor coordination deficit but no learning or memory impairment. These results suggest that *Rhes* disruption affects selected behavioral competencies.

The thyroid hormones thyroxine (T_4) and triiodothyronine (T_3) have many physiological effects. They exert their actions in all tissues examined and affect many metabolic pathways. Some of the most prominent effects of thyroid hormones occur during fetal development and in early childhood. In humans, the lack of adequate levels of thyroid hormones in the first trimester of life, such as in iodine deficiency (endemic cretinism) (8, 9), or in developmental abnormalities of the thyroid gland (congenital hypothyroidism) (22, 28, 55) results in cretinism, a syndrome of severe mental deficiency, which may be accompanied by retarded growth and/or neurological deficits, such as spastic diplegia. Many of these developmental effects are not reversed by later treatment with hormone, indicating that thyroid hormone acts in a specific developmental window. Therefore, adequate levels of thyroid hormone are required for normal central nervous system development.

To date, several specific central nervous system genes whose expression is controlled by thyroid hormone have been identified. The expression of these genes may be decreased (2, 5) or increased (1, 18) in hypothyroidism. Furthermore, the total or partial absence of thyroid hormones may also affect either mRNA stability (43, 54) or the mRNA translational process (43, 57, 60). The identification of thyroid hormone target genes in the central nervous system and the understanding of their function in central nervous system development are important to understanding the pathogenesis of neurological cretinism at the molecular level.

In order to understand the molecular basis of neurological cretinism, we studied the *Rhes* (Ras homolog enriched in striatum) gene (24). *Rhes* is predominantly expressed in the striatum, and its expression is controlled by thyroid hormones (59). Interestingly, several lines of evidence indicate that in neurological cretinism, there is damage of striatum, which determines a striatopallidal syndrome with poor motor coordination and spastic diplegia (8, 9, 39).

Rhes, composed of 266 amino acids, belongs to the RASD subfamily of the Ras-related GTP-binding protein superfamily. Rhes has 95% identity with TEM2 (58) and 62% identity with Dexras1 (37), which are other members of the RASD subfamily. Ras family proteins are molecular switches that respond to extracellular signals and regulate intracellular signal pathways controlling cell growth (40, 41), gene transcription (20, 61), mRNA stability and translation (7, 15, 52), cytoskeleton organization (33, 38), peptide trafficking (23, 46, 50), and secretion (3, 45). In the central nervous system, Ras protein controls pathways that are involved in synaptic plasticity, learning, and memory (10).

To assess the role of Rhes in mature striatum and in the pathogenesis of neurological cretinism, we generated mice carrying null mutations in the *Rhes* gene by a gene-targeting method. In this paper, we show that mice homozygous for the *Rhes* mutation are viable and fertile but smaller than wild-type mice. Furthermore, they show a gender-dependent increase in anxiety levels and a motor coordination deficit but no learning or memory impairment.

MATERIALS AND METHODS

Tissue preservation and histological analysis. Mice were killed by CO_2 asphyxiation. Brains and embryos were isolated, fixed, and embedded in paraffin as described previously (19). Brains were cut in 10-μm sections; embryos were cut in 7-μm sections. In situ hybridization was carried out on paraffin-embedded sections as described previously (19). The *Rhes* riboprobe was transcribed from a 372-bp AflII-PvuII genomic fragment of the 3′ untranslated region located 42

* Corresponding author. Mailing address: Stazione Zoologica Anton Dohrn, Villa Comunale, 80121 Naples, Italy. Phone: 39 081 5833278. Fax: 39 081 5833258. E-mail: rdilauro@unina.it.

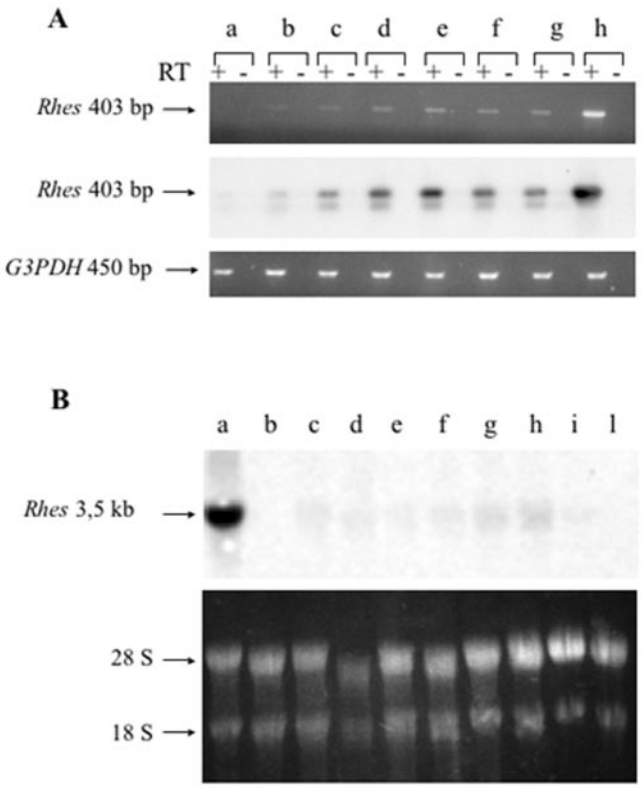

FIG. 1. *Rhes* expression profile during embryo development and in the adult mouse. (A) (Top panel) RT-PCR analysis performed with total RNAs prepared from E12.5 (a), E13.5 (b), E14.5 (c), E15.5 (d), E16.5 (e), E17.5 (f), and E18.5 (g) embryo brains. Total RNA from adult brain (h) was used as a positive control for PCR. The oligonucleotides were designed according to the sequence of the mouse *Rhes* gene and amplified a 403-bp fragment of the *Rhes* 3′ untranslated region. (Middle panel) Specificity of PCR products checked by hybridization with a 207-bp PstI-NcoI fragment derived from the *Rhes* sequence between the PCR primers. (Bottom panel) G3PDH gene amplification performed as an internal control for RT-PCR. (B) (Upper panel) Northern blot performed with total RNAs prepared from mouse adult tissues (brain [a], liver [b], kidney [c], thyroid [d], lung [e], heart [f], and testis [g]) and TL5 (h), R1 (i), and MEF (l) cells. The probe used was the 372-bp AflII-PvuII fragment of the mouse *Rhes* genomic locus, located 42 bp downstream of the translational stop codon. The lower panel shows the 28S and 18S rRNAs of each sample.

bp downstream of the *Rhes* stop codon. The *EGFP* (enhanced green fluorescent protein) riboprobe was transcribed from a 747-bp NcoI-BamHI fragment, which contains all of the *EGFP* coding region.

RNA analysis. Total RNA was isolated from adult mouse tissues, staged embryos brains, and cultured cells by the guanidine hydrochloride procedure as previously described (16); 5 μg of total RNA, previously treated with RNase-free DNase I (Roche), was used for reverse transcription (RT)-PCR analysis. Reverse transcription of mRNAs was carried out with the SuperScript preamplification system for first-strand cDNA synthesis (Life Technologies). Single-stranded cDNAs in 2 μl of a 25-μl reaction mixture were amplified by PCR with *Taq* DNA polymerase (Roche). Glyceraldehyde-3-phosphate dehydrogenase (G3PDH) mRNA was amplified as an internal control for the reverse transcription reaction. The oligonucleotide primers used were *Rhes* (5′-ACTAGTTCAGGACA GAGCTCTGAC-3′ and 5′-CAGCAGGTGTCTTTATCCAGAGTC-3′) and *G3PDH* (5′-TCCACCACCCTGTTGCTGTA-3′ and 5′-ACCACAGTCCAT GCCATCAC-3′). For Northern blot analysis, 15 μg of total RNA was separated on a 1% formaldehyde–agarose gel, blotted onto a Hybond N nylon membrane (Amersham), and hybridized with the 372-bp AflII-PvuII genomic fragment labeled with ^{32}P.

Rhes antibody preparation. The sequence encoding full-length rat Rhes, included between the NdeI and EcoRV sites, was cloned in the NdeI site and filled-in BamHI site of vector pET15b; the full-length protein fused with a 6His stretch at its NH_2 terminus (6H-Rhes) was expressed in *Escherichia coli* BL21(DE3). The protein was solubilized in 4 M urea and injected into rabbits (30). The anti-Rhes antiserum was purified by affinity chromatography as previously described (19).

Western blot analysis. Total protein extracts from wild-type and knockout striatum and from transfected cells were prepared as previously described (34), resolved by sodium dodecyl sulfate (SDS)–4 to 15% polyacrylamide gel electrophoresis (PAGE) on a precast gel (Bio-Rad), and transferred to a polyvinylidene difluoride membrane (Millipore). As a positive control, HeLa cells were transfected with the Pb-Rhes construct, encoding Rhes protein under the control of the *PGK-1* promoter. The blot was probed with a 1:20,000 dilution of polyclonal anti-Rhes antibody and developed with the ECL Plus Western blotting detection reagent (Amersham Life Science).

Generation of knockout mice. The *Rhes* genomic locus was isolated by PCR screening of the phage artificial chromosome library RPCI-21 (provided by the Yac Screening Center, DIBIT-HSR and IGBE-CNR, Milan, Italy). The internal ribosome entry site-EGFP cassette and the *PGKneo* cassette, flanked by *loxP* sequences, were flanked by two *Rhes* genomic DNA fragments: a 2.9-kb fragment including the *Rhes* translational start codon and a 5-kb fragment (see Fig. 3A). The 2.9-kb genomic fragment underwent a site-directed mutagenesis reaction which allowed insertion of a stop codon in each reading frame and EcoRI and XhoI restriction sites downstrea of the *Rhes* translational start codon. The site-directed mutagenesis reaction was performed with the QuikChange site-directed mutagenesis kit (Stratagene) according to the manufacturer's instructions.

The oligonucleotide primers used for the mutagenesis reaction were 5′-CTT AGCAGGCACCTCGAGTGTGGAATTCCTACTGGACTAGGTCTTCATC ATG-3′ and 5′-CATGATGAAGACCTAGTCCAGTAGGAATTCCACACTC GAGGTGCCTGCTAAG-3′. The herpes simplex virus thymidine kinase cassette was positioned downstream of the 3′ homology arm. Transfection of the targeting vector and selection of the mutant embryonic stem (ES) cells (R1) were performed as described previously (21) except that 400 μg of G418 (Gibco) per ml was used. Screening of ES cell clones and genotyping of mice were carried out by Southern blot analysis. Genomic DNA samples were digested with EcoRI or StuI; the 0.8-kb KpnI and 0.55-kb KpnI-StuI fragments, located outside the homology arms, were used as probes (see Fig. 4A for probe positions and digestion product sizes). Embryo manipulations and aggregations of ES cell clones with mouse blastocysts of strain CD1 were carried out as described previously (36). Chimeric animals with a high contribution of the 129/Sv genetic background, as judged from coat color, were bred with CD1 mice. Offspring heterozygous for the disrupted *Rhes* gene were mated to each other to produce *Rhes* null mice.

Thyroid-stimulating hormone, glucose, and amylase measurements. Thyroid-stimulating hormone levels in blood collected from wild-type and knockout mice on postnatal days 30 and 180 were analyzed with a rat thyroid-stimulating hormone radioimmunoassay kit (Amersham). The glucose levels in blood collected from wild-type and knockout mice on postnatal day 120 were analyzed as described previously (49). Amylase levels were analyzed as described previously (29).

Animals. Ten adult (five males and five females) wild-type mice and 10 adult (five males and five females) knockout mice were used in all experiments. The wild-type mice were generated from crosses of the heterozygous mice to have the same genetic background as the $Rhes^{-/-}$ mice. The animals were housed in an air-conditioned room (temperature, 21 ± 1°C; relative humidity, 60 ± 10%) with the lights on from 2000 to 0800 h, in Plexiglas boxes (33 by 13 by 14 cm) with a metal top and sawdust as bedding. Pellet food (enriched standard diet, purchased from Mucedola, Settimo Milanese, Milan, Italy) and tap water were continuously available. Before each test, mice were individually weighed. For the Morris water maze test, they were weighed both the first day, before testing, and the last day, after testing.

Behavioral tests. The tests below were carried out according to the references given in parentheses: open-field (14), passive avoidance (13, 17), elevated plus-maze (35, 53), rota-rod (11), and Morris water maze (12, 42).

Statistical analysis. Analyses of variance were performed on body weight, duration, and frequency data in each behavioral category measured in the open-field and elevated plus-maze tests and on learning performance data for the Morris water maze. Post hoc comparisons were performed by Tukey's Honestly Significantly Different test. In the passive avoidance test, Mann-Whitney analysis was applied to evaluate the main effect of treatment and Wilcoxon analysis to evaluate the main effect of sex. In the rota-rod test, in order to assess the significance of the difference between wild-type and knockout mice, the Mann-

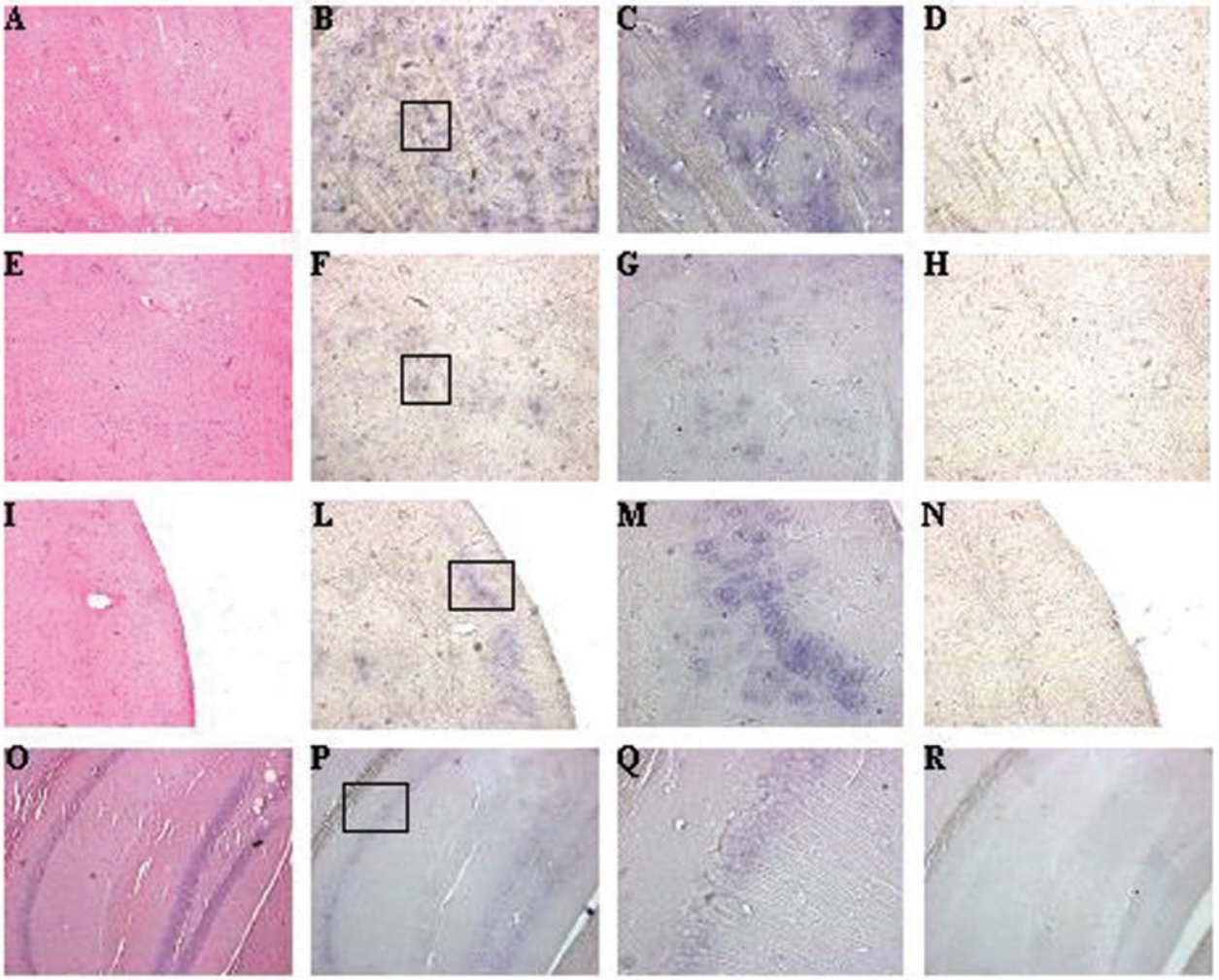

FIG. 2. *Rhes* expression in adult brain. Sagittal sections of CD1 adult mouse brain: striatum (A, B, C, and D), accumbens nucleus (E, F, G, and H), olfactory tubercle and piriform cortex (I, L, M, and N), and hippocampus (O, P, Q, and R). Sections A, E, I, and O were stained with hematoxylin and eosin; sections B, C, F, G, L, M, P, and Q were hybridized to the *Rhes* antisense riboprobe; sections D, H, N, and R were hybridized to the *Rhes* sense riboprobe. Sections C, G, M, and Q was higher magnifications of sections B, F, L, and P, respectively.

Whitney *U* test was used. The main effect of speed was analyzed by the Friedman nonparametric analysis of variance, and Wilcoxon analysis was used to evaluate the main effect of sex. When no main effect of sex and/or genotype × sex interactions was found, the sex variable was not considered in the analysis.

RESULTS

Expression of *Rhes* during brain development and in adult tissues. We analyzed the expression pattern of *Rhes* in the developing mouse brain by RT-PCR. Total RNA was extracted from the brains of CD1 staged embryos. RT-PCR analysis detected *Rhes* mRNA starting from embryonic day 13.5 (E13.5) (Fig. 1A). We analyzed the expression pattern of *Rhes* in CD1 adult mouse tissues by Northern blot analysis. *Rhes* was expressed at very high levels in brain and at low levels in kidney, thyroid, lung, heart, and testis (Fig. 1B). No *Rhes* mRNA was detected in liver. A low level of *Rhes* expression was also detected in the rat thyroid cell line FRTL-5 and in the mouse ES cell line R1 (44) (Fig. 1B). Since R1 cells were grown on mouse embryonic fibroblasts (MEFs), we also analyzed *Rhes* expression in MEF cells. The absence of the hybridization band in total RNA from MEF cells demonstrated bona fide *Rhes* expression in ES cells and not in the MEF layer.

To obtain further insights into the distribution of *Rhes* mRNA during embryogenesis and in the adult brain, we performed in situ hybridization experiments (Fig. 2). *Rhes* mRNA was prominently expressed in the striatum, but it was also present in the accumbens nucleus (ventral part of striatum), in the olfactory tubercle, in the piriform cortex, and in the hippocampus dentate gyrus. No signal was detected with a *Rhes* sense riboprobe. Surprisingly, no signal was detected by in situ hybridization in the brain of E15.5 and E17.5 embryos, suggesting that, during embryogenesis, *Rhes* mRNA levels are below the limit of detection of our in situ hybridization technique.

Targeting of the mouse *Rhes* locus. In order to inactivate the *Rhes* locus, we constructed a targeting vector (Fig. 3A). The 5′ homology arm was mutagenized to insert a stop codon in each frame immediately downstream of the *Rhes* translational start

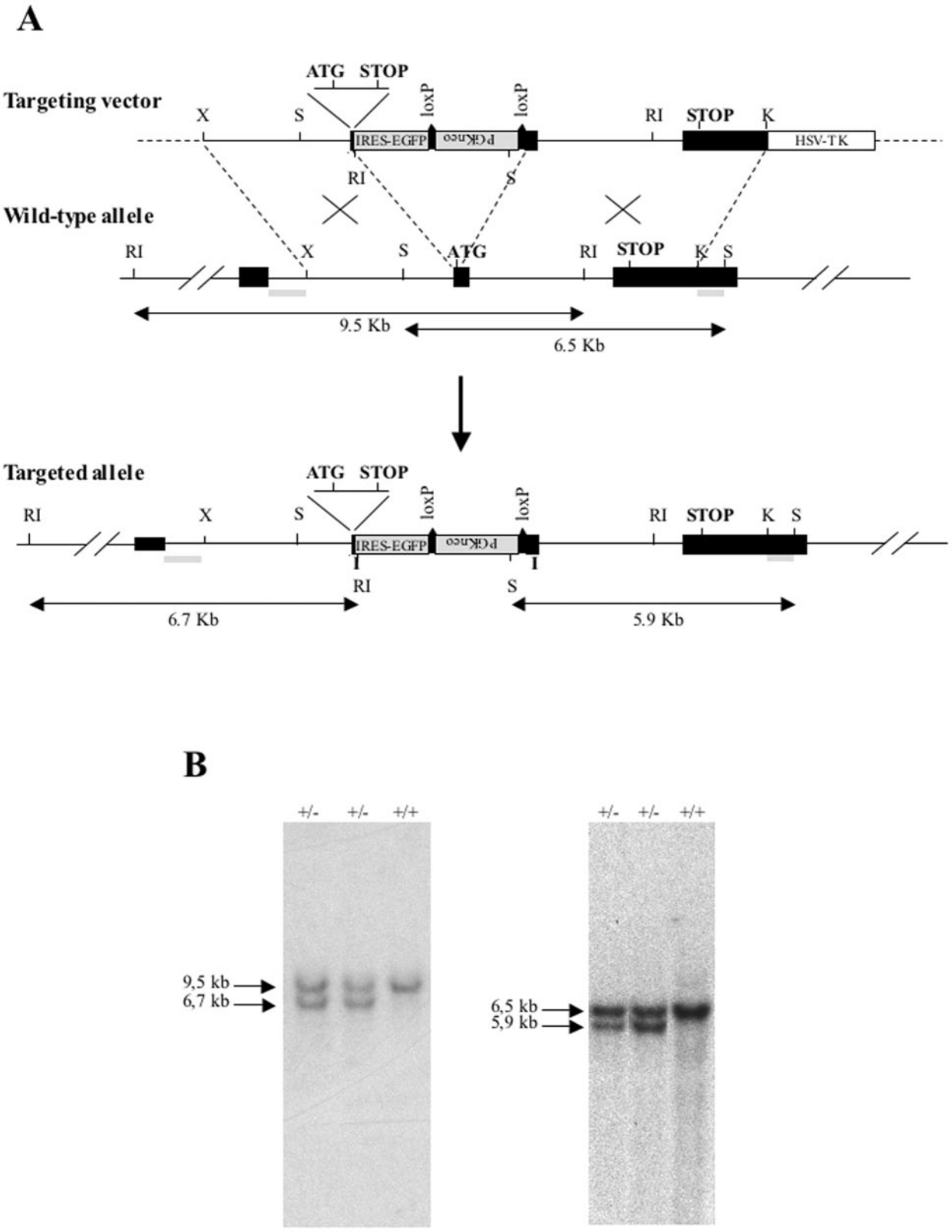

FIG. 3. (A) Homologous recombination in ES cells. Targeting vector and wild-type and mutant *Rhes* allele maps are shown. Restriction enzyme sites and probes (represented as boxes located upstream and downstream of the homologous arms) are shown. The fragments obtained from wild-type and mutant allele digestions are also shown. K, KpnI; X, XbaI; S, StuI; RI, EcoRI. (B) Identification of ES cell recombinant clones by Southern blot analysis. Left panel: DNA isolated from ES cell clones was digested with EcoRI and probed with a 0.8-kb KpnI fragment (located 5′ to the genomic fragment for homologous recombination), yielding 9.5-kb and 6.7-kb bands for the wild-type and targeted alleles, respectively. Right panel: Homologous recombination was confirmed by digesting DNA from positive clones with StuI and probing it with a 0.55-kb KpnI-StuI fragment (located 3′ to the genomic fragment for homologous recombination), yielding 6.5- and 5.9-kb bands for the wild-type and targeted alleles, respectively. +/+, wild type; +/−, *Rhes*$^{+/-}$.

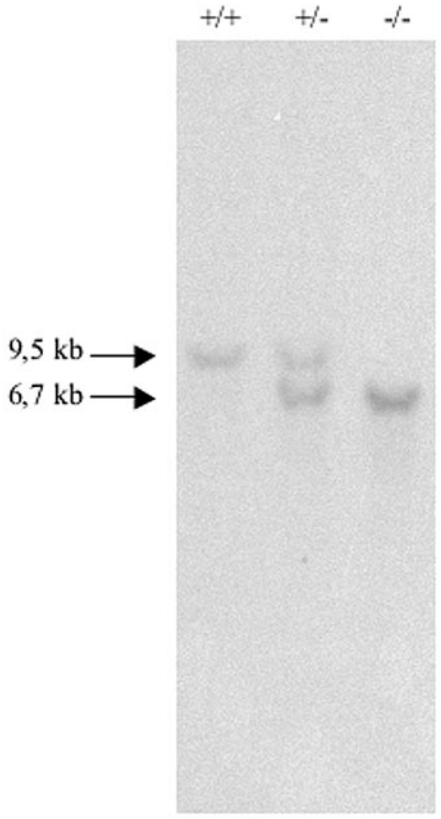

FIG. 4. Identification of knockout mice. Southern blot analysis of offspring generated from mating of mice heterozygous for the *Rhes* null mutation. DNA isolated from tails was digested with EcoRI and probed with a 0.8-kb KpnI fragment, yielding 9.5- and 6.7-kb bands for the wild-type and targeted alleles, respectively. +/+, wild type; +/−, $Rhes^{+/-}$; −/−, $Rhes^{-/-}$.

codon. The targeting vector contained the internal ribosome entry site-EGFP cassette and *PGKneo* cassette flanked by *loxP* sequences between the homology arms (6). Furthermore, the construct was flanked by a cassette for the herpes simplex virus thymidine kinase gene for negative selection. The targeting vector was designed to abolish the synthesis of Rhes and to place the *EGFP* coding sequence downstream of the *Rhes* regulatory sequences (Fig. 3A). The targeting construct was transfected into RI ES cells, and the recombinant clones were identified by Southern blot analysis (Fig. 3B). Chimeric mice were generated with five independently targeted ES cell clones. In the progeny of one chimera, we obtained 48 ES cell-derived animals (agouti), of which 27 carried the wild-type *Rhes* allele and the remainder carried the targeted *Rhes* allele, consistent with a Mendelian pattern of transmission.

Rhes protein is not essential for normal embryo development. To assess whether *Rhes* function is essential for normal development, we interbred $Rhes^{+/-}$ mice. The heterozygous mice were fertile; each mating was productive, and the litter sizes were indistinguishable from those obtained with wild-type mice. The genotypes of the newborns were assessed by Southern blot analysis (Fig. 4). Of 117 mice examined, 28 were wild type, 67 were heterozygous, and 22 were homozygous for the mutant allele. The ratio of the three classes of animals was not significantly different from the expected values for normal transmission of the wild-type and mutant alleles. The $Rhes^{-/-}$ mice were viable, showing that the *Rhes* gene product does not play a vital role, at least in the CD1 background. Furthermore, mice homozygous for the *Rhes* knockout allele mated and were fertile, and the litter sizes were indistinguishable from those of wild-type and heterozygous matings.

In situ hybridization and Western blot analysis on knockout mouse brain. To determine *Rhes* expression in $Rhes^{-/-}$ mice, we performed in situ hybridization experiments and Western blot analyses. Since the main *Rhes* expression site was the striatum, we focused on this region of the brain. In situ hybridization showed that *Rhes* mRNA was barely detectable in the striatal region of the knockout mouse brain (Fig. 5), while it was clearly detected in wild-type animals. We also carried out an in situ hybridization experiments with an antisense riboprobe of *EGFP* because, in the targeting vector, the *EGFP* gene was controlled by the *Rhes* promoter. Figure 5 shows that *EGFP* mRNA was detected in the striatum of the $Rhes^{-/-}$ mouse. No signal was detected with the sense riboprobes for either *Rhes* or *EGFP*.

To explore the presence of the Rhes protein, we prepared a rabbit anti-Rhes polyclonal antibody. We proved the efficacy and the specificity of the antibody by Western blotting on HeLa cell extracts transfected with either a Rhes expression vector or an empty vector. Rhes protein was only detected in the cells transfected with the Rhes expression vector (Fig. 6, lane c) while no cross-reacting proteins were seen in the control extracts (Fig. 6, lane d). However, Western blotting carried out on striatum protein extracts with the same antibody revealed the presence of protein bands that were present both in wild-type (Fig. 6, lane b) and knockout (Fig. 6, lane a) animals that we interpreted as nonspecific. Three bands were present only in the wild-type mice and were completely absent in knockout extracts. The lower band displayed a mobility very similar to that of Rhes expressed in HeLa cells. The slight difference could be due to different posttranslational modifications happening in the in vitro and in vivo models. The upper bands identified proteins of higher molecular mass. Interestingly, the Rhes locus shows several transcripts, one of which (accession number BC036988) encodes a protein containing Rhes at the C terminus and extending 48 additional amino acids at the N terminus without an initiator methionine, suggesting that the actual protein could be longer, like the one(s) that we detected in the Western blot.

Taking together the RNA and protein data on Rhes expression, we conclude that the targeted Rhes allele presented in this paper does not produce any detectable Rhes protein. We have also presented evidence of a novel Rhes-related protein whose presence was also abolished in the knockout mouse that we generated.

Rhes affects body weight. We observed that knockout mice weighed less than wild-type mice, as clearly shown by a significant main effect of genotype [$F_{(1, 16)} = 9.247$ and $P = 0.0078$; see Fig. 8]. Furthermore, a genotype-age interaction [$F_{(2, 32)} = 3.487$ and $P = 0.0427$] but not a genotype-sex interaction was found. At each age analyzed (postnatal days 70, 100, and 130), a marked weight difference between wild-type and knockout mice in both males and females was revealed by post hoc analysis ($P < 0.01$; Fig. 7). Since *Rhes* is expressed in the

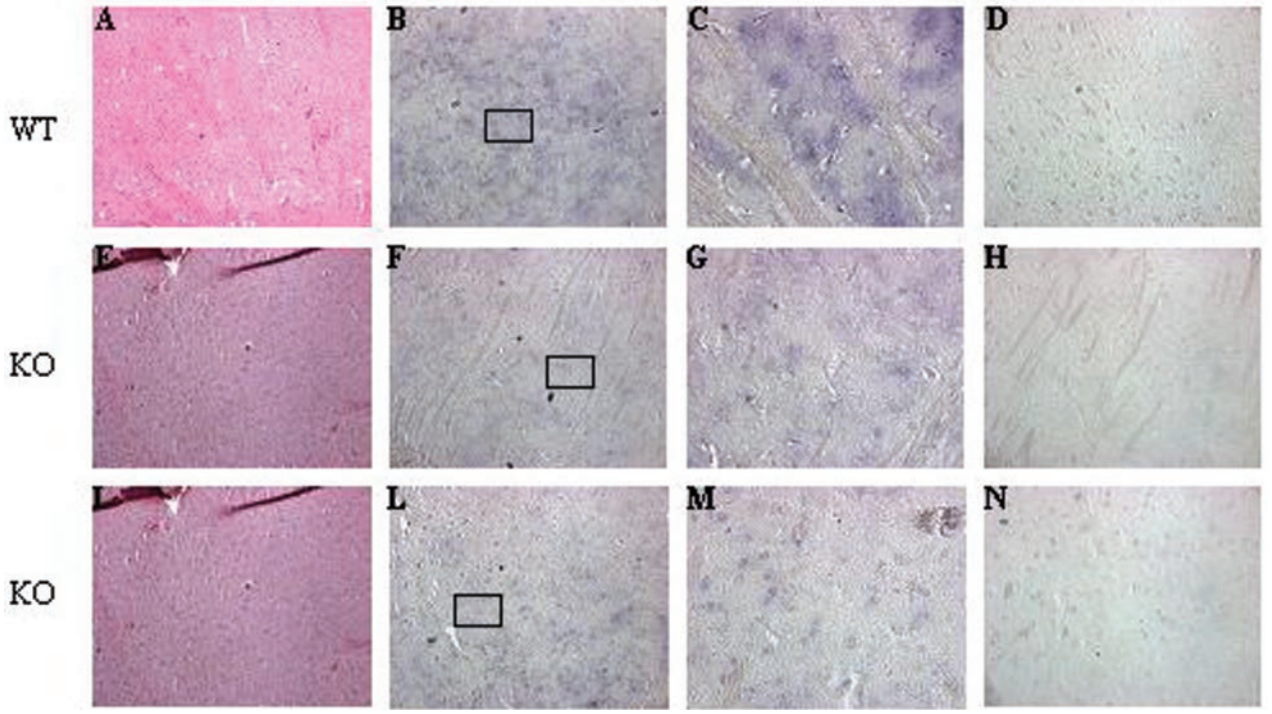

FIG. 5. *Rhes* and *EGFP* expression in knockout mouse brain. The in situ hybridization experiments were carried out on sagittal sections of adult mouse brain from CD1 (wild type [WT]) (sections A, B, C, and D) and *Rhes*$^{-/-}$ (knockout [KO]) (sections E, F, G, H, I, L, M, and N) mice. Sections A, E, and I were stained with hematoxylin and eosin; sections B, C, F, and G were hybridized to the *Rhes* antisense riboprobe; sections D and H were hybridized to the *Rhes* sense riboprobe; sections L and M were hybridized to the *EGFP* antisense riboprobe; section N was hybridized to the *EGFP* sense riboprobe. Sections C, G, and M are higher magnifications of sections B, F, and L, respectively.

thyroid gland and in pancreatic β-cells (14bis), we tested the thyroid-stimulating hormone, glucose, and amylase levels in age-matched homozygous knockout and wild-type mice. No statistically significant differences were found (data not shown).

Behavioral analysis of *Rhes*$^{-/-}$ mice. (i) Passive avoidance and Morris water maze tests. In both the passive avoidance and Morris water maze tests, no significant difference between wild-type and knockout mice was found (data not shown).

(ii) Open-field test. In the first 15 min of the open-field test test, no main effect of genotype was found in distance moved, and the genotype × 5-min block interaction missed statistical significance [$F_{(2, 36)} = 2.704$ and $P = 0.0805$; Fig. 8]. However, post hoc comparison revealed that knockout mice had an altered locomotor profile, moving less than wild-type mice during the first 5 min (post hoc, $P < 0.05$; Fig. 8).

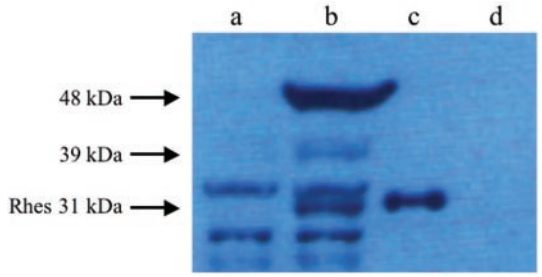

FIG. 6. Expression of Rhes protein in wild-type and *Rhes*$^{-/-}$ striatum. *Rhes*$^{-/-}$ (a) and wild-type (b) striatum protein extracts (100 μg of total protein/lane) were analyzed by Western blotting with anti-Rhes polyclonal antibody; 0.4 μg of total protein from HeLa cells transfected with a Rhes construct (c) was used as the positive control; and 0.4 μg of total protein from HeLa cells transfected with the empty vector (d) was used as the negative control. Arrows indicate proteins present in wild-type and absent in knockout extracts.

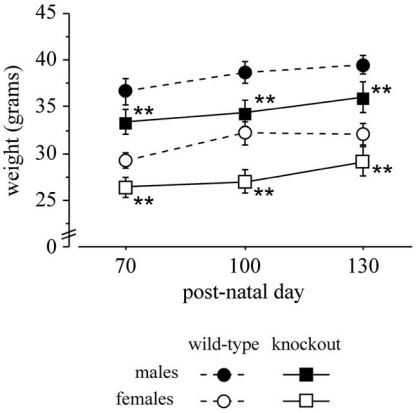

FIG. 7. Body weights of wild-type and knockout mice measured on postnatal days 70, 100, and 130. Data are means ± standard error of the mean, $n = 5$. The double asterisk indicates a significant difference between wild-type and knockout mice ($P < 0.01$).

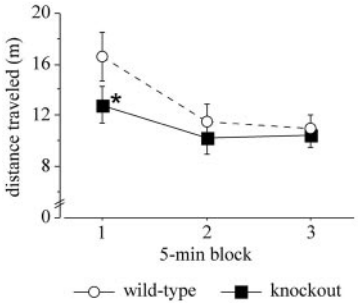

FIG. 8. Locomotor activity in the open-field test. The distance traveled by wild-type and knockout mice is shown. Data are means ± standard error of the mean. Data for males and females were pooled ($n = 10$). The asterisk indicates a significant difference between wild-type and knockout mice ($P < 0.05$).

(iii) Elevated plus-maze test. In agreement with previous studies (26, 51), wild-type males displayed higher anxiety levels than wild-type females in the elevated plus-maze test. This profile was found inverted in knockout mice, females being more anxious than males, as illustrated by a significant genotype × sex interaction observed in the following measures (Fig. 9): percent of open arm entries [$F_{(1, 16)} = 7.011$ and $P = 0.0175$], number of open arm entries [$F_{(1, 16)} = 4.438$ and $P = 0.0500$], percent of time spent in the open arms [$F_{(1, 16)} = 5.059$ and $P = 0.0389$], and percent of time spent in the closed arms [$F_{(1, 16)} = 4.878$ and $P = 0.0421$]. In the last measure, a clear difference between wild-type and knockout females was evident (post hoc, $P < 0.05$), indicating abnormally high anxiety levels in knockout females compared to wild-type females. Other measures confirmed increased anxiety levels in knockout mice, especially in knockout females (Fig. 9). A significant genotype-sex interaction was observed in percent of head-dipping [$F_{(1, 16)} = 6.347$ and $P = 0.0228$] and percent of stretch attend postures [$F_{(1, 16)} = 5.998$ and $P = 0.0262$], both performed in the protected area. Moreover, knockout mice showed less locomotion than wild-type mice, spending a long time in immobility [$F_{(1, 16)} = 4.336$ and $P = 0.0500$]. It is worth noting that four knockout mice (two males and two females) out of 10 fell from the plus-maze during the test, while none of the wild-type mice did ($P < 0.05$; Fisher test).

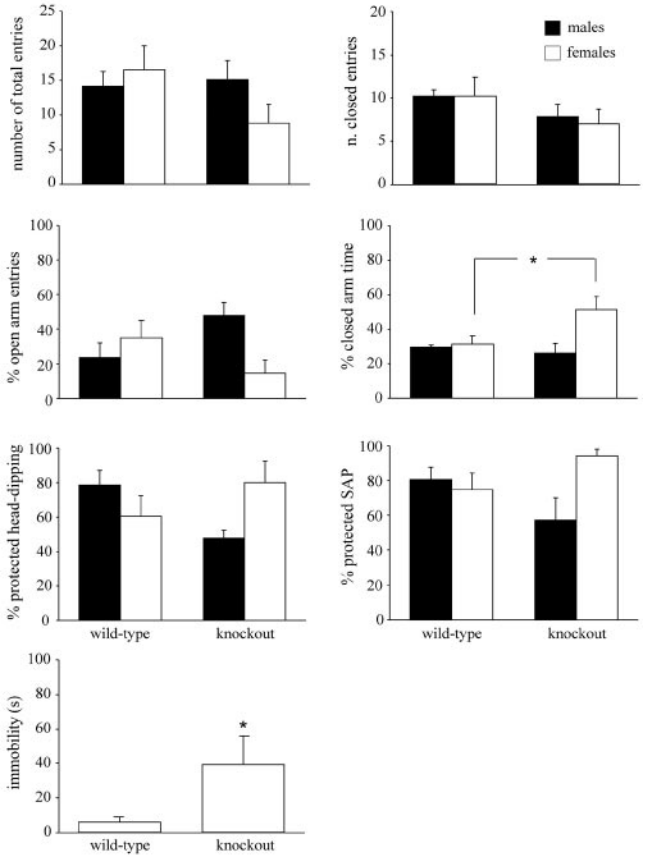

FIG. 9. Behavioral endpoints in the plus-maze test. The number of total and closed arm entries, the percentage of open arm entries, the percentage of closed arm time, the percentage of protected head dipping and stretch attend postures, and immobility shown by wild-type and knockout mice are indicated. Data are means ± standard error of the mean ($n = 5$). For immobility, data for males and females were pooled ($n = 10$). The asterisk indicates a significant difference between wild-type and knockout mice ($P < 0.05$).

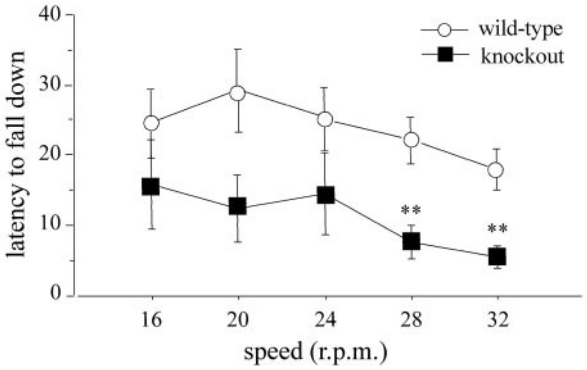

FIG. 10. Balance and motor coordination in the rota-rod test. The time before falling at each speed level shown by wild-type and knockout mice is indicated. Data are means ± standard error of the mean. Data for males and females were pooled ($n = 10$). The double asterisk indicates a significant difference between wild-type and knockout mice ($P < 0.01$).

(iv) Rota-rod test. In the rota-rod test, though both genotypes displayed a similar over-trial profile, decreasing their tendencies to fall from the mast with the increase in speed (Friedman χ^2 in the overall group = 17.73, $P = 0.0014$), knockout mice always had worse performances than wild-type mice (main effect of genotype; Mann-Whitney $U = 81.5$, $P = 0.0172$) (Fig. 10). Specifically, knockout mice fell within significantly shorter times at the two fastest speeds (post hoc, $P < 0.01$).

DISCUSSION

The mechanism responsible for impairment of brain function in thyroid hormone deficiencies is not well understood. It is known that several genes in the brain are under thyroid hormone control, but it is not clear which gene(s), when deregulated, is responsible for the phenotype observed in thyroid hormone deficiencies or how it does so. In this study we focused on the role of *Rhes*, a gene under thyroid hormone

control that is expressed in the striatum. Rhes is a member of a new subfamily of Ras-related small GTP-binding proteins recently identified. To this end, we generated mice homozygous for the *Rhes* null mutation. We checked the absence of Rhes protein in the knockout mouse striatum by Western blot analysis. This analysis also showed the absence of another protein which probably originates from the *Rhes* locus by alternative transcription initiation and splicing.

The knockout mice were viable, and their general condition did not reveal gross abnormalities with the exception of a reduced body weight. The macroscopic analysis of adult tissues which express Rhes did not show any gross abnormalities between knockout and wild-type mice. The knockout animals mated and were fertile, and the litter sizes were indistinguishable from those of wild-type matings. No alteration of thyroid and pancreatic gland functions was observed, even though *Rhes* is expressed in the wild-type glands. Given that the absence of thyroid hormone determines severe damage to the developing striatum in neurological cretinism (8, 9, 39), we analyzed in detail the behavioral features of *Rhes* knockout mice. These mice showed a significant decrease in locomotor activity compared to wild-type mice. Interestingly, *Rhes* deletion influenced the anxiety response in the plus-maze test in a gender-specific manner. The impact of gender on the anxiety test has been widely studied in mice, and in the plus-maze test, females generally show lower anxiety levels than males (35, 48). In the present study, wild-type mice behaved as expected, while an opposite trend has been found in $Rhes^{-/-}$ mice, females showing higher anxiety levels than males in most of the endpoints considered.

The main behavioral effect of *Rhes* deletion was a marked impairment in motor coordination. In particular, knockout mice showed a clear impairment in the rota-rod test. This task has been proven to be very sensitive to striatum integrity (11, 25, 56) and has also been used to detect the progressive decline of striatal function in R6/2 Huntington gene transgenic mice (27, 31). Thus, the motor coordination impairment shown by *Rhes* knockout mice in the rota-rod test, confirmed by the number of falls in the plus-maze, is strongly concordant with the main striatal localization of the Rhes protein (24, 59).

The striatum is reportedly involved in cognitive abilities, from motor planning to reward seeking and procedural learning (4, 32). Consistent with the role played by the striatum in motor activity and learning processes, these abilities are dramatically impaired in advanced Parkinson's disease (47). *Rhes* knockout mice showed no learning or memory impairment in the water maze and passive avoidance tests, suggesting that Rhes protein may be involved only in selected striatal processes not influencing learning and memory. This finding indicates that mental retardation linked to hypothyroidism may be independent of alteration in *Rhes* levels or function.

In conclusion, the modest behavioral deficits of *Rhes* knockout mice indicate that *Rhes* is involved in selected striatal competencies, mainly locomotor activity and motor coordination, suggesting that its downregulation in hypothyroidism could be responsible only for a subset of symptoms, such as the striatopallidal syndrome (8, 9, 39).

ACKNOWLEDGMENTS

We thank Mario De Felice for advice in generation of knockout mice and Giovanni Maraviglia for technical assistance. We also thank Tommaso Russo for glucose and amylase determination and Andreas Nagy for providing the R1 ES cell line.

This work was supported in part by Telethon grant GP0208Y01, by a grant from the Associazione Italiana per la Ricerca sul Cancro (to R.D.L.), by Ministero dell'Università e della Ricerca Scientifica e Tecnologica grant "I geni dell'uomo" cluster 01, and by Italian Ministry of Health project ALZ1 (to E.A.). A.R., M.T.P., P.M., and A.A. were supported by Biogem s.c.a.r.l., Italy.

REFERENCES

1. **Alvarez-Dolado, M., J. M. Gonzalez-Sancho, J. Bernal, and A. Munoz.** 1998. Developmental expression of the tenascin-C is altered by hypothyroidism in the rat brain. Neuroscience **84:**309–322.
2. **Alvarez-Dolado, M., T. Iglesias, A. Rodriguez-Pena, J. Bernal, and A. Munoz.** 1994. Expression of neurotrophins and the trk family of neurotrophin receptors in normal and hypothyroid rat brain. Brain Res. Mol. Brain Res. **27:**249–257.
3. **Baldini, G., G. Wang, M. Weber, M. Zweyer, R. Bareggi, J. W. Witkin, and A. M. Martelli.** 1998. Expression of Rab3D N135I inhibits regulated secretion of ACTH in AtT-20 cells. J. Cell Biol. **140:**305–313.
4. **Berke, J. D., and S. E. Hyman.** 2000. Addiction, dopamine, and the molecular mechanisms of memory. Neuron **25:**515–532.
5. **Bernal, J., J. Numez.** 1995. Thyroid hormones and brain development. Eur. J. Endocrinol. **4:**390–398.
6. **Betz, U. A., C. A. Vosshenrich, K. Rajewsky, and W. Muller.** 1996. Bypass of lethality with mosaic mice generated by Cre-loxP-mediated recombination. Curr. Biol. **6:**1307–1316.
7. **Birnberg, N. C., P. J. Stork, and L. M. Hemmick.** 1992. Expression of the c-Harvey ras oncogene alters peptide synthesis in the neurosecretory cell line AtT20. J. Biol. Chem. **267:**15464–15468.
8. **Boyages, S. C.** 1993. Clinical review 49: Iodine deficiency disorders. J. Clin. Endocrinol. Metab. **77:**587–591.
9. **Boyages, S. C., and J. P. Halpern.** 1993. Endemic cretinism: toward a unifying hypothesis. Thyroid **3:**59–69.
10. **Brambilla, R., N. Gnesutta, L. Minichiello, G. White, A. J. Roylance, C. E. Herron, M. Ramsey, D. P. Wolfer, V. Cestari, C. Rossi-Arnaud, S. G. Grant, P. F. Chapman, H. P. Lipp, E. Sturani, and R. Klein.** 1997. A role for the Ras signaling pathway in synaptic transmission and long-term memory. Nature **390:**281–286.
11. **Brandon, E. P., S. F. Logue, M. R. Adams, M. Qi, S. P. Sullivan, A. M. Matsumoto, D. M. Dorsa, J. M. Wehner, G. S. McKnight, and R. L. Idzerda.** 1998. Defective motor behavior and neural gene expression in RIIbeta-protein kinase A mutant mice. J. Neurosci. **18:**3639–3649.
12. **Calamandrei, G., A. Venerosi, I. Branchi, and E. Alleva.** 1999. Effects of prenatal zidovudine treatment on learning and memory capacities of preweanling and young adult mice. Neurotoxicology **20:**17–25.
13. **Calamandrei, G., A. Venerosi, I. Branchi, F. Chiarotti, A. Verdina, F. Bucci, and E. Alleva.** 1999. Effects of prenatal AZT on mouse neurobehavioral development and passive avoidance learning. Neurotoxicol. Teratol. **21:**29–40.
14. **Calamandrei, G., A. Venerosi, I. Branchi, A. Valanzano, and E. Alleva.** 2000. Prenatal exposure to anti-HIV drugs. long-term neurobehavioral effects of lamivudine (3TC) in CD-1 mice. Neurotoxicol. Teratol. **22:**369–379.
15. **Chandler, L. A., C. P. Ehretsmann, and S. Bourgeois.** 1994. A novel mechanism of Ha-*ras* oncogene action: regulation of fibronectin mRNA levels by a nuclear posttranscriptional event. Mol. Cell. Biol. **14:**3085–3093.
16. **Chomczynski, P., and N. Sacchi.** 1987. Single-step method of RNA isolation by acid guanidinium thiocyanate-phenol-chloroform extraction. Anal. Biochem. **162:**156–159.
17. **Costa, L. G., and S. D. Murphy.** 1982. Passive avoidance retention in mice tolerant to the organophosphorus insecticide disulfoton. Toxicol. Appl. Pharmacol. **65:**451–458.
18. **Cuadrado, A., J. Bernal, and A. Munoz.** 1999. Identification of the mammalian homolog of the splicing regulator Suppressor-of-white-apricot as a thyroid hormone regulated gene. Brain Res. Mol. Brain Res. **71:**332–340.
19. **Dathan, N., R. Parlato, A. Rosica, M. De Felice, and R. Di Lauro.** 2002. Distribution of the titf2/foxe1 gene product is consistent with an important role in the development of foregut endoderm, palate, and hair. Dev. Dyn. **224:**450–456.
20. **Davis, R. J.** 1995. Transcriptional regulation by MAP kinases. Mol. Reprod. Dev. **42:**459–467.
21. **De Felice, M., C. Ovitt, E. Biffali, A. Rodriguez-Mallon, C. Arra, K. Anastassiadis, P. E. Macchia, M. G. Mattei, A. Mariano, H. Scholer, V. Macchia, and R. Di Lauro.** 1998. A mouse model for hereditary thyroid dysgenesis and cleft palate. Nat. Genet. **19:**395–398.
22. **Dugbartey, A. T.** 1998. Neurocognitive aspects of hypothyroidism. Arch. Intern. Med. **158:**1413–1418.

23. **Ellis, S., and H. Mellor.** 2000. Regulation of endocytic traffic by rho family GTPases. Trends Cell Biol. **10:**85–88.
24. **Falk, J. D., P. Vargiu, P. E. Foye, H. Usui, J. Perez, P. E. Danielson, D. L. Lerner, J. Bernal, and J. G. Sutcliffe.** 1999. Rhes: A striatal-specific Ras homolog related to Dexras1. J. Neurosci. Res. **57:**782–788.
25. **Fernagut, P. O., S. Chalon, E. Diguet, D. Guilloteau, F. Tison, and M. Jaber.** 2003. Motor behaviour deficits and their histopathological and functional correlates in the nigrostriatal system of dopamine transporter knockout mice. Neuroscience **116:**1123–1130.
26. **Fernandes, C., M. I. Gonzalez, C. A. Wilson, and S. E. File.** 1999. Factor analysis shows that female rat behaviour is characterized primarily by activity, male rats are driven by sex and anxiety. Pharmacol. Biochem. Behav. **64:**731–738.
27. **Ferrante, R. J., O. A. Andreassen, B. G. Jenkins, A. Dedeoglu, S. Kuemmerle, J. K. Kubilus, R. Kaddurah-Daouk, S. M. Hersch, and M. F. Beal.** 2000. Neuroprotective effects of creatine in a transgenic mouse model of Huntington's disease. J. Neurosci. **20:**4389–4397.
28. **Fisher, D. A.** 1991. Clinical review 19: management of congenital hypothyroidism. J. Clin. Endocrinol. Metab. **72:**523–529.
29. **Guilbault, G. G., and E. B. Rietz.** 1976. Enzymatic, fluorometric assay of alpha-amylase in serum. Clin. Chem. **22:**1702–1704.
30. **Harlow, E., and D. Lane.** 1988. Antibodies: a laboratory manual. Cold Spring Harbor Laboratory Press, Cold Spring Harbor, N.Y.
31. **Hockly, E., P. M. Cordery, B. Woodman, A. Mahal, A. van Dellen, C. Blakemore, C. M. Lewis, A. J. Hannan, and G. P. Bates.** 2002. Environmental enrichment slows disease progression in R6/2 Huntington's disease mice. Ann. Neurol. **51:**235–242.
32. **Hyman, S. E., and R. C. Malenka.** 2001. Addiction and the brain: the neurobiology of compulsion and its persistence. Nat. Rev. Neurosci. **2:**695–703.
33. **Johnson, D. I.** 1999. Cdc42: an essential Rho-type GTPase controlling eukaryotic cell polarity. Microbiol. Mol. Biol. Rev. **63:**54–105.
34. **Johnson, L., D. Greenbaum, K. Cichowski, K. Mercer, E. Murphy, E. Schmitt, R. T. Bronson, H. Umanoff, W. Edelmann, R. Kucherlapati, and T. Jacks.** 1997. K-ras is an essential gene in the mouse with partial functional overlap with N-ras. Genes Dev. **11:**2468–2481.
35. **Johnston, A. L., and S. E. File.** 1991. Sex differences in animal tests of anxiety. Physiol. Behav. **49:**245–250.
36. **Joyner, A. L.** 2000. Gene targeting: a practical approach, 2nd ed.
37. **Kemppainen, R. J., and E. N. Behrend.** 1998. Dexamethasone rapidly induces a novel ras superfamily member-related gene in AtT-20 cells. J. Biol. Chem. **273:**3129–3131.
38. **Kjoller, L., and A. Hall.** 1999. Signaling to Rho GTPases. Exp. Cell Res. **253:**166–179.
39. **Ma, T., Z. C. Lian, S. P. Qi, E. R. Heinz, and G. R. DeLong.** 1993. Magnetic resonance imaging of brain and the neuromotor disorder in endemic cretinism. Ann. Neurol. **34:**91–94.
40. **Maruta, H., H. He, A. Tikoo, T. Vuong, and E. K. M. Nur.** 1999. G proteins, phosphoinositides, and actin-cytoskeleton in the control of cancer growth. Microsc. Res. Tech. **47:**61–66.
41. **McCormick, F.** 1995. Ras-related proteins in signal transduction and growth control. Mol. Reprod. Dev. **42:**500–506.
42. **Morris, R.** 1984. Developments of a water-maze procedure for studying spatial learning in the rat. J. Neurosci. Methods **11:**47–60.
43. **Munoz, A., A. Rodriguez-Pena, A. Perez-Castillo, B. Ferreiro, J. G. Sutcliffe, and J. Bernal.** 1991. Effects of neonatal hypothyroidism on rat brain gene expression. Mol. Endocrinol. **5:**273–280.
44. **Nagy, A., J. Rossant, R. Nagy, W. Abramow-Newerly, and J. C. Roder.** 1993. Derivation of completely cell culture-derived mice from early-passage embryonic stem cells. Proc. Natl. Acad. Sci. USA **90:**8424–8428.
45. **Ngsee, J. K., A. M. Fleming, and R. H. Scheller.** 1993. A rab protein regulates the localization of secretory granules in AtT-20 cells. Mol. Biol. Cell **4:**747–756.
46. **Novick, P., and M. Zerial.** 1997. The diversity of Rab proteins in vesicle transport. Curr. Opin. Cell Biol. **9:**496–504.
47. **Olanow, C. W., and W. G. Tatton.** 1999. Etiology and pathogenesis of Parkinson's disease. Annu. Rev. Neurosci. **22:**123–144.
48. **Palanza, P.** 2001. Animal models of anxiety and depression: how are females different? Neurosci. Biobehav. Rev. **25:**219–233.
49. **Palomba, S., T. Russo, F. Orio, Jr., A. Sammartino, F. M. Sbano, C. Nappi, A. Colao, P. Mastrantonio, G. Lombardi, and F. Zullo.** 2004. Lipid, glucose and homocysteine metabolism in women treated with a GnRH agonist with or without raloxifene. Hum. Reprod. **19:**415–421.
50. **Pfeffer, S. R.** 1994. Rab GTPases: master regulators of membrane trafficking. Curr. Opin. Cell Biol. **6:**522–526.
51. **Pryce, C. R., J. Lehmann, and J. Feldon.** 1999. Effect of sex on fear conditioning is similar for context and discrete CS in Wistar, Lewis and Fischer rat strains. Pharmacol. Biochem. Behav. **64:**753–759.
52. **Riis, B., S. I. Rattan, B. F. Clark, and W. C. Merrick.** 1990. Eukaryotic protein elongation factors. Trends Biochem. Sci. **15:**420–424.
53. **Rodgers, R. J., and N. J. Johnson.** 1995. Factor analysis of spatiotemporal and ethological measures in the murine elevated plus-maze test of anxiety. Pharmacol. Biochem. Behav. **52:**297–303.
54. **Rodriguez-Pena, A., N. Ibarrola, M. A. Iniguez, A. Munoz, and J. Bernal.** 1993. Neonatal hypothyroidism affects the timely expression of myelin-associated glycoprotein in the rat brain. J. Clin. Investig. **91:**812–818.
55. **Rosman, N. P.** 1972. The neuropathology of congenital hypothyroidism. Adv. Exp. Med. Biol. **30:**337–366.
56. **Sedelis, M., R. K. Schwarting, and J. P. Huston.** 2001. Behavioral phenotyping of the MPTP mouse model of Parkinson's disease. Behav. Brain Res. **125:**109–125.
57. **Silva, J. E., and P. Rudas.** 1990. Effects of congenital hypothyroidism on microtubule-associated protein-2 expression in the cerebellum of the rat. Endocrinology **126:**1276–1282.
58. **St Croix, B., C. Rago, V. Velculescu, G. Traverso, K. E. Romans, E. Montgomery, A. Lal, G. J. Riggins, C. Lengauer, B. Vogelstein, and K. W. Kinzler.** 2000. Genes expressed in human tumor endothelium. Science **289:**1197–1202.
59. **Vargiu, P., B. Morte, J. Manzano, J. Perez, R. de Abajo, J. Gregor Sutcliffe, and J. Bernal.** 2001. Thyroid hormone regulation of rhes, a novel Ras homolog gene expressed in the striatum. Brain Res. Mol. Brain Res. **94:**1–8.
60. **Walker, P., M. E. Weichsel, Jr., D. Eveleth, and D. A. Fisher.** 1982. Ontogenesis of nerve growth factor and epidermal growth factor in submaxillary glands and nerve growth factor in brains of immature male mice: correlation with ontogenesis of serum levels of thyroid hormones. Pediatr. Res. **16:**520–524.
61. **Wasylyk, B., J. Hagman, and A. Gutierrez-Hartmann.** 1998. Ets transcription factors: nuclear effectors of the Ras-MAP-kinase signaling pathway. Trends Biochem. Sci. **23:**213–216.